



**HAL**  
open science

## Exploring the inhibition of targeted microalgae by a *Cylindrotheca closterium* nonaxenic biofilm

Lucie Sanchez, Amandine Avouac, Emilie Le Floc'H, Christine Félix,  
Christophe Leboulanger, Angélique Gobet, Eric Fouilland

► **To cite this version:**

Lucie Sanchez, Amandine Avouac, Emilie Le Floc'H, Christine Félix, Christophe Leboulanger, et al..  
Exploring the inhibition of targeted microalgae by a *Cylindrotheca closterium* nonaxenic biofilm. 2024.  
hal-04662985v1

**HAL Id: hal-04662985**

**<https://hal.science/hal-04662985v1>**

Preprint submitted on 26 Jul 2024 (v1), last revised 13 Dec 2024 (v2)

**HAL** is a multi-disciplinary open access archive for the deposit and dissemination of scientific research documents, whether they are published or not. The documents may come from teaching and research institutions in France or abroad, or from public or private research centers.

L'archive ouverte pluridisciplinaire **HAL**, est destinée au dépôt et à la diffusion de documents scientifiques de niveau recherche, publiés ou non, émanant des établissements d'enseignement et de recherche français ou étrangers, des laboratoires publics ou privés.

1 **Exploring the inhibition of targeted microalgae by a *Cylindrotheca closterium* non-**  
2 **axenic biofilm**

3

4 Lucie Sanchez, Amandine Avouac, Emilie le Floc'h, Christine Félix, Christophe Leboulanger,  
5 Angélique Gobet and Eric Fouilland\*

6

7 MARBEC, Univ Montpellier, CNRS, Ifremer, IRD, Sète, France

8 \*corresponding author: eric.fouilland@cnrs.fr

9

10 **Abstract** Monospecific microalgal dominance in nutrient-rich environments is usually  
11 attributed to exclusive resource competition or grazing selectivity. However, allelopathic  
12 interactions within microalgal communities may reinforce established dominance and limit  
13 species replacement. While many allelopathic interaction studies among autotrophic  
14 microorganisms focused on aquatic free-living species, scarce knowledge exists on  
15 microalgae aquatic biofilms, although chemical communication between species or  
16 communities is favored due to spatial proximity. We thus developed and applied a co-culture  
17 protocol using a disc diffusion method to evidence the inhibitory potential of biofilms of the  
18 marine diatom *Cylindrotheca closterium* growing in non-axenic conditions on different  
19 targeted microalgal strains. The biofilm exhibited an inhibitory effect on the individual  
20 growth of two microalgal strains, *Nannochloropsis oculata* and *Tetraselmis striata*, but did  
21 not affect the microalga *Porphyridium purpureum*. Bacteria isolated from the inhibition zone  
22 did not show any inhibitory activity on targeted microalgae. This suggests that the growth  
23 inhibition and cell deformation observed for the two sensitive microalgal strains may result  
24 from compounds produced during the growth of *C. closterium* biofilm or from associated  
25 bacteria identified but not isolated in the present study. Therefore, further investigations are  
26 required to identify the compounds and their microbial producers involved in the observed  
27 inhibition.

28

29 **Keywords** Microalgae, Allelopathic interactions, Biofilm, Bacteria, Microbial co-culture

30

31

32 **Introduction**

33

34 The dominance of microalgal species in a nutrient-rich environment may be explained by  
35 exclusive resource competition or grazing selectivity (Vallina et al. 2014). However,  
36 interactions within algal communities may also occur by allelopathy (Legrand et al. 2003),  
37 defined as a chemical communication involved in inter-species competition, where one  
38 species prevents other organisms from using available resources by producing effective  
39 molecules. Distinguishing competition from allelopathy under natural conditions remains  
40 difficult (Inderjit and del Moral 1997). If competition is mainly characterized by the species  
41 intrinsic ability for resource acquirement, the allelopathic effects depend on the sensitivity  
42 and physiological status of the targeted organism, the distance between the emitter and the  
43 target, and the concentration of produced molecules (Leflaive and Ten-Hage 2007).  
44 Therefore, allelopathic interactions are particularly expected in aquatic biofilms because  
45 organisms are physically close (Allen et al. 2016). When lipophilic, allelochemical  
46 compounds can readily diffuse through extracellular polymeric substances constituting  
47 biofilm matrix, or direct cell-to-cell contact, reducing their dilution. Their concentration can  
48 therefore be significant in the biofilm while being less detectable in the surrounding water  
49 (Allen et al. 2016, Uchida 2001). Allelopathic compounds may be produced to target  
50 planktonic organisms. In this case, these molecules must be sufficiently concentrated to affect  
51 targets over greater distances in a diluted aquatic environment (Gross 2003).

52 Diatoms are species known for the production of inhibitory compounds, such as  
53 polyunsaturated fatty acids (PUFAs), polyunsaturated aldehydes (PUAs), polyphenolic and  
54 halogenated compounds that have been proven to negatively impact other microalgae  
55 (Pichierri et al. 2017; Wenjing et al. 2019). The marine diatom *Cylindrotheca closterium*,  
56 living both as free-floating cells or in biofilm, displays allelopathy abilities when cultured in  
57 planktonic form (Wenjing et al. 2019). However, the allelopathy ability of *C. closterium*  
58 when growing in biofilm is unknown.

59 Most studies investigating microalgal vs microalgal allelopathy used non-axenic  
60 cultures and filtered growth medium dissolved fractions, without considering the ability of  
61 bacteria to produce inhibitory or algicidal compounds in the biofilm (Coyne et al. 2022), and  
62 some of the allelopathic compounds required to be continuously produced to be effective  
63 (Flores et al. 2012). The inhibitory activity of microalgal biofilms against potential  
64 competitors may be a valuable trait when cultivating commercially relevant microalgal  
65 species. Attached culture systems, an emerging technology replacing suspended culture  
66 systems, facilitate biomass growth as a biofilm on a support continually rotating between  
67 liquid and gaseous phases (Morales et al. 2020). Recent works highlighted the reduction of

68 environmental impact of such new production systems (Morales et al. 2020, Penaranda et al.  
69 2023). The long-term growth of microalgae in attached culture systems showing very little  
70 microalgal contaminations during growing periods (F. Guiheneuf, personal communication),  
71 suggests potential allelopathy ability.

72

73 We therefore hypothesized that microalgae and associated bacteria established in  
74 biofilm under favorable growth conditions may have the ability to inhibit potential  
75 competitors such as allochthonous microalgae. To test this hypothesis, we examined the  
76 inhibitory potential of the diatom *Cylindrotheca closterium*'s biofilm when cultivated using  
77 this attached culture system under laboratory conditions. Inhibition tests were performed  
78 using experimental *C. closterium* biofilm co-cultures from a modified version of the disc  
79 diffusion method (Hudzicki 2009) against three selected microalgae targets. Two of the  
80 studied targets are pelagic and marine microalgae, *Tetraselmis striata* and *Nannochloropsis*  
81 *oculata*, from the Chlorophyta and Ochrophyta family, respectively. The third studied target  
82 was a benthic microalga of marine origin, the red microalga, *Porphyridium purpureum* from  
83 the Rhodophyta family. These microalgae were selected for inhibition tests because they can  
84 grow on biofilm, and they belong to genera that are susceptible to be inhibited through  
85 allelochemicals such as *Tetraselmis* and *Nannochloropsis* (Khairy 2010, Chaïb et al. 2021) or  
86 less sensitive to allelochemicals such as *Porphyridium purpureum* (Hellio et al. 2002). In  
87 addition, those strains belong to different taxonomic divisions, promoting a broad  
88 representation of biological diversity, as well as a diversity of size, morphology, and  
89 pigments.

90

91

92

## 93 **Materials and methods**

94

95

### 96 **Microalgae strains**

97

98 The benthic diatom *Cylindrotheca closterium* AC170 was obtained from the Algobank Caen  
99 Collection (Université de Caen Basse-Normandie, France) and used as a potential emitter.  
100 Three marine non-axenic microalgal strains from three algal lineages were chosen as targets,  
101 for a broader representation of biological diversity, as well as diversity in size, morphology,

102 and physiology. The selected strains were: i) the planktonic chlorophyte *Tetraselmis striata*  
103 isolated and identified in 2018 from a high-rate algal pond located in Palavas-les-flots  
104 (Southern France, Pascon et al. 2021), ii) the planktonic ochrophyte *Nannochloropsis oculata*  
105 (CCAP 847/9) and iii) the benthic rhodophyte *Porphyridium purpureum* (CCAP 1380).

106

### 107 **Culture conditions**

108

109 Before experimentations, the four microalgal strains were cultured in planktonic mode using a  
110 modified f/2 medium (Guillard and Ryther 1962, Guillard 1975, Supl. Table 1), prepared with  
111 Instant Ocean (Aquarium Systems) adjusted to achieve a salinity of 40 g.L<sup>-1</sup>. All cultures  
112 were incubated at 20 °C under continuous white light with a light intensity of 85 μmol  
113 photons m<sup>-2</sup>.s<sup>-1</sup>.

114 *Cylindrotheca closterium* was cultivated as a biofilm using a small rotating  
115 experimental culture system (Figure 1) under controlled laboratory conditions (controlled  
116 temperature of 20 °C and light of 80-90 μmol photons.m<sup>-2</sup>.s<sup>-1</sup>) with weekly sterile culture  
117 medium addition (modified f/2 medium with twice the concentration in nitrogen, phosphate  
118 and silicate, using synthetic sea salts Instant Ocean adjusted to reach a salinity of 40 g.L<sup>-1</sup>). A  
119 plastic tank (L35 cm x W25 cm x H15 cm) was used and contained a roller with a length of  
120 30 cm and a diameter of 10 cm, with a rotating bar allowing for tangential velocity ranging  
121 from 0.02 to 0.07 m.s<sup>-1</sup>. A textile fabric was autoclaved and placed on the roller using zip ties.  
122 On March 10<sup>th</sup> 2023, the fabric was moistened on the roller with a sterile culture medium for  
123 one day and inoculated by evenly pouring onto the fabric the planktonic culture of *C.*  
124 *closterium* at 5.7 rotations per minute (rpm) under a light intensity of 90 μmol photons m<sup>-2</sup>.s<sup>-1</sup>.  
125 The plastic tank was then half-filled with 3.6 L of sterile culture medium, ensuring that ¾ of  
126 the roller was exposed to the air while ¼ was immersed in the culture medium. After 10 days  
127 and visual check of signs of biofilm establishment, the rotation speed was increased to 15 rpm  
128 and the light intensity was raised to 100 μmol photons m<sup>-2</sup>.s<sup>-1</sup> in order to ensure higher access  
129 to light and nutrients without risking biofilm detachment. Once the biofilm onto the fabric  
130 reached maturity after three weeks (characterized by a dark brown colour, uniformity, and  
131 opacity, see Fig. 1A), it was collected by scraping the entire fabric. After the first harvest  
132 from the fabric, the rotation speed was increased to 37 rpm, equivalent to a linear speed of 0.2  
133 m s<sup>-1</sup> that is the optimal speed before inducing too much shearing and friction forces that will  
134 lead to cell detachment (F. Guiheneuf, personal communication). The entire biofilm was  
135 harvested every three weeks. The biofilm that developed at the bottom of the tank was

136 harvested every week before fresh culture medium renewal (Figure 1A). The harvested one-  
137 week biofilm at the bottom of the tank after 14 days of experiment (March 24<sup>th</sup> 2023,  
138 hereafter referred to as 14T) and after 131 days of experiment (July 19<sup>th</sup> 2023, 131T) and the  
139 harvested three-week biofilm from the fabric on the roller after 131 days of experiment  
140 (131R) were tested for potential inhibition on targeted microalgae strains.

141

#### 142 **Inhibition tests using *Cylindrotheca closterium* biofilm on targeted microalgae**

143 Inhibition tests were developed based on the paper disc antibiotic sensitivity testing design, to  
144 visualize the formation of an inhibition halo against a microalgal target spread on a Petri dish,  
145 from a disc on which *C. closterium* biofilm was deposited. To get homogeneous targeted  
146 microalgal mats, and for each of the targeted microalga, a sterile cotton swab with 6 mm  
147 cotton wool tip was dipped into the planktonic microalgae culture in the exponential growth  
148 phase and streaked onto the 1.5% agar-containing modified f/2 medium by making tight  
149 streaks. For each targeted species, one such Petri dish was used as a control and three others  
150 for the inhibition tests. Sterile cellulosic discs were then arranged on the agar surface. One  
151 disc was inoculated with 20  $\mu\text{L}$  of positive control (35% hydrogen peroxide), another disc  
152 with 20  $\mu\text{L}$  of negative control (sterile modified f/2 medium), a third disc was inoculated with  
153 the *C. closterium* biofilm and two other discs were inoculated after centrifuging the *C.*  
154 *closterium* biofilm at 4500 g for 10 minutes at 20 °C. A volume of 20  $\mu\text{L}$  was deposited on  
155 each disc with the respective pellet and raw supernatant of *C. closterium*. Centrifugation  
156 intended to separate the particulate from the dissolved fractions of the biofilm. Filtration at  
157 0.2  $\mu\text{m}$  using polycarbonate filter was also performed from *C. closterium* biofilm on roller  
158 fabric. The one-week biofilm of *C. closterium* that was developing at the bottom of the tank  
159 was sampled after 14 days and after 131 days of experiment, while the three-week *C.*  
160 *closterium* biofilm formed on the roller fabric was scraped after 131 days. After placing the  
161 two controls and biofilms onto the cellulosic discs, the Petri dishes were all incubated in  
162 duplicates for 15 days at 20 °C under continuous white light at an intensity of 85  $\mu\text{mol}$   
163  $\text{photons.m}^{-2}.\text{s}^{-1}$ . After 15 days of incubation, when present, the diameters of the inhibition  
164 zones were measured and observed under the inverted microscope to evaluate the  
165 physiological condition of the cells. Statistical analyses comparing means were conducted  
166 using a Mann-Whitney test on cell dimension measurements, with a significance level set at a  
167  $p$ -value of 0.05.

168

#### 169 **Bacteria isolates from inhibition zones**

170 The potential role of bacteria in the inhibition activity was investigated. When inhibition  
171 zones around cellulosic discs were observed, samples were taken with an oese to isolate and  
172 identify the bacterial strains from these zones and to perform additional inhibition tests on  
173 targeted microalgae. Bacteria were isolated using serial dilutions (1/10, 1/100 and 1/1000),  
174 and then spread on Zobell agar medium to isolate colonies. The Petri dishes were incubated  
175 for eight days at 20 °C in the dark. Dilutions (1/10 or 1/100) that allowed the maximum  
176 number of identifiable bacterial colonies were preserved. Morphologically distinct colonies  
177 were isolated on new duplicated plates and incubated at 20°C in the dark until obtaining  
178 distinct and separate colonies (between 48 hours and 120 hours, depending on the bacterial  
179 strain). Individual colonies were then sub-cultured onto a new plate and incubated under the  
180 same conditions at least two more times to ensure strain purity.

181 The identification of isolated bacterial strains was carried out using a Sanger  
182 sequencing approach. A heat shock was performed on the bacterial cultures frozen at -20 °C,  
183 to a temperature of 95 °C for 15 minutes to access their DNA. Amplification of the 16S  
184 rRNA gene of each bacterial colony was then performed using universal primers: forward 8F  
185 (5'-AGAGTTTGATCCTGGCTCAG-3'; Edwards *et al.* 1989) and reverse 1492R (5'-  
186 CGGTTACCTTGTTACGACTT-3'; Stackebrandt and Liesack, 1993). A reaction mixture  
187 was prepared with: 4 µL of GoTaq buffer 1X, 0.4 µL dNTP at a final concentration of 0.2  
188 mM each, 1 µL of each primer at a final concentration of 0.5 µM, 0.1 µL of GoTaq DNA  
189 polymerase 1.25 U (Promega, city), 12.5 µL of molecular-grade water, and 1 µL of bacterial  
190 DNA for a final volume of 20 µL per reaction. The PCR reaction was carried out according to  
191 the following program: initial denaturation for 2 minutes at 95 °C, 30 cycles of 30 seconds at  
192 95 °C for denaturation, 45 seconds at 55 °C for hybridization, and 1 minute at 72 °C for  
193 extension, followed by a final extension step of 4 minutes at 72 °C. To validate the  
194 amplification of the 16S rRNA gene, an agarose gel of 0.9% in 1X Tris Acetate EDTA (TAE)  
195 buffer was prepared in 50 ml, and 2 µL of a DNA intercalating dye (Biotium, Gelred, 1/4  
196 concentration) were added. The gel was placed in an electrophoresis chamber (Advance,  
197 Mupid-One) containing 1X TAE. Five microliters of each PCR product with 1 µL of 10X  
198 loading buffer (Invitrogen, Bluejuice) were loaded into the wells and allowed to migrate for  
199 30 minutes at 100 volts. The gels were then observed under ultraviolet light in a gel reader.  
200 When a band around 1.5 Kb was visible, which corresponds to the expected size for the  
201 amplification of 16S rRNA gene, 2 µL of Exosap-IT Express were added to 5 µL of each  
202 PCR product to purify them and retain only the amplicons (removal of primers and excess  
203 dNTP). The mixture was incubated for 4 minutes at 37 °C to allow enzyme treatment,

204 followed by 1 minute at 80 °C to inactivate it. The DNA concentration of each purified PCR  
205 product was measured by spectrophotometry using a Nanodrop (ND-1000  
206 spectrophotometer). A dilution was then performed to obtain a DNA concentration of 10  
207 ng.µL<sup>-1</sup>. Five microliters of the 8F primer at a concentration of 5 pmol.µL<sup>-1</sup> were added to the  
208 purified amplicons before sending them to Eurofins Genomics for sequencing of the first half  
209 of the 16S rDNA. Once the amplicons were sequenced, the quality of the obtained  
210 electropherograms was observed using the Bioedit software version (Hall, 1999). Sequences  
211 were compared to the GenBank database of the National Center for Biotechnology  
212 Information (NCBI) using the BLAST search program to establish a preliminary  
213 determination of their taxonomy. For each sequence, all hits with a sequence coverage greater  
214 than 99%, a sequence identity percentage greater than 97%, and an E-value of 0 were  
215 retained. The isolated strain *Alteromonas macleodii*, isolated from the inhibition zone  
216 obtained using centrifuged *T. striata* biofilm supernatant (see Table 2), was then tested at  
217 different cell concentrations (10<sup>6</sup>, 10<sup>7</sup>, 10<sup>8</sup> cell.ml<sup>-1</sup>) against targeted microalgae strains to  
218 check for potential growth inhibition using the same diffusion test protocol as described in the  
219 previous paragraph.

220

### 221 **Identification of the bacterial community in the biofilm**

222 To identify the bacterial community from the biofilm of the experimental culture system, we  
223 further used a metabarcoding approach on the samples from the bottom of the tank on March  
224 24<sup>th</sup> (14T) and July 19<sup>th</sup> 2023 (131T), and from the roller fabric on the same date (131R).  
225 DNA was extracted from the 3 biofilm samples using the DNeasy PowerBiofilm Kit  
226 (Qiagen). The V3-V4 variable region of the 16S rRNA gene was amplified using a primer set  
227 designed to avoid the amplification of chloroplastic 16S rRNA gene: S-D-Bact-0341-b-S-17:  
228 CCTACGGGNGGCWGCAG as forward and 799F\_rc: CMGGGTATCTAATCCKGTT as  
229 reverse (Klindworth et al. 2013; Thomas et al. 2020). The PCR reaction mix was composed of  
230 12,5µL of KAPA HiFi HotStart ReadyMix 2X (KapaBiosystems), 0.75 µL of each primer at  
231 a final concentration of 0.3 µM, 9 µL of molecular-grade water, and 2 µL of bacterial DNA  
232 (2ng uL<sup>-1</sup>) for a final volume of 25 µL per reaction. PCR were carried out using the  
233 following program: initial denaturation for 3 minutes at 95 °C, 10 cycles of [30 sec at 95 °C,  
234 45 sec at 44 °C, and 90 sec at 68 °C], and 15 cycles of [20 sec at 94 °C, 45 sec at 50 °C, and  
235 90 sec at 68 °C], followed by a final extension step of 4 minutes at 68 °C. Negative controls  
236 were used for the sampling, DNA extraction and PCR steps to control for potential  
237 contaminants. PCR were performed in triplicate and then pooled before metabarcoding.



238 Amplicons were then sent to the GeT-Biopuces platform for index addition, MiSeq Illumina  
239 sequencing (Run MiSeq 600 cycles V3) and sequence processing using the dada2 package  
240 (Callahan et al. 2016) in R (R Core Team, 2021). Sequence processing included removal of  
241 sequences with N, of low quality and of size below 100 bp, and filtration of the phiX  
242 sequences. It also included sequence dereplication, ASV formation and chimera removal.  
243 Taxonomic annotation was done using Silva version v138.1 (Quast et al. 2013) and GTDB  
244 r202 (Parks et al. 2022). Before further analyses, the ASV table was transformed by  
245 normalizing the number of sequences using median sequencing depth (Trefault et al. 2021).

246

## 247 **Results**

248

### 249 **Microalgal inhibition from *Cylindrotheca closterium* biofilm**

250

251 A zone of inhibition was observed from the one-week *C. closterium* biofilm collected at the  
252 bottom of the tank, on the microalgal targets *N. oculata* and *T. striata* (Figure 2). The  
253 percentages of inhibition relative to the positive control (hydrogen peroxide) for *N. oculata*  
254 and *T. striata* varied respectively between 65 to 158% and between 24 and 92%, according to  
255 the type of biofilm sample (i.e. pellet, supernatant, or whole) and days of experiment (Table  
256 1). However, no zone of inhibition was observed for the target *P. purpureum* for the three  
257 types of biofilm sample. Zones of inhibition on the *N. oculata* and *T. striata* targets was also  
258 observed when *C. closterium* grown on fabric was used as emitter. The percentages of  
259 inhibition relative to the positive control for *N. oculata* and *T. striata* varied respectively  
260 between 16 to 39% and between 12 to 38%, according to the three types of biofilm sample  
261 (Table 1). These inhibition activities seemed to be lower than that measured using the bottom  
262 tank biofilm (Table 1). No inhibition was observed on these targeted algal strains when  
263 filtered (0.2  $\mu\text{m}$ ) centrifuged biofilm supernatant was used as an emitter.

264 Samples were taken from the diffusion tests in the inhibition zones and observed  
265 under an inverted microscope. Regarding the targeted microalgae *N. oculata*, we observed the  
266 presence of *C. closterium* cells in the samples taken from the inhibition zone of the paste, the  
267 pellet, and the supernatant. From the inhibition zones, different sizes of *N. oculata* cells were  
268 observed (Figure 3A) compared to *N. oculata* cultivated without any discs (control culture).  
269 In the inhibition zone, one population of *N. oculata* with cells significantly larger than the  
270 control culture (Mann Whitney,  $n=20$ ,  $p$ -value < 0.05) was observed with an average size of  
271  $5.07 \pm 0.09 \mu\text{m}$ , and a second population of *N. oculata* was also observed with cells

272 significantly smaller than the control culture (Mann Whitney, n=20,  $p$ -value < 0.05) with an  
273 average size of  $1.76 \pm 0.10 \mu\text{m}$ . In comparison, *N. oculata* population in the control culture  
274 had an average cell size of  $2.90 \pm 0.08 \mu\text{m}$ . In these inhibition zones, we did not observe a  
275 significant change (Mann Whitney, n=20,  $p$ -value > 0.05) in the length of *C. closterium* cells  
276 ( $50.9 \pm 0.3 \mu\text{m}$ ) in comparison to the *C. closterium* control, i.e. *C. Closterium* growing alone  
277 on Petri dish ( $51.6 \pm 0.2 \mu\text{m}$ ). However, we observed a significant decrease in the diameter of  
278 the *C. closterium* cells, with a diameter of  $5.70 \pm 0.10 \mu\text{m}$  for the control culture and  $4.23 \pm$   
279  $0.11 \mu\text{m}$  for the samples taken from the inhibition zone (Mann Whitney, n=20,  $p$ -value <  
280 0.05). Regarding the targeted microalgae *T. striata*, we also observed the presence of *C.*  
281 *closterium* in all the inhibition zones. Two types of *T. striata* cells were observed: one with an  
282 average size of  $11.07 \pm 0.16 \mu\text{m}$ , similar to the diameter of the control culture ( $10.90 \pm 0.18$   
283  $\mu\text{m}$ , Mann Whitney, n=20,  $p$ -value > 0.05), and a second type of cells with a significantly  
284 smaller average size of  $4.60 \pm 0.09 \mu\text{m}$  (Mann Whitney, n=20,  $p$ -value < 0.05). *T. striata* cells  
285 with a significantly smaller size than the control also showed membrane deformation (Figure  
286 3B). As observed in the *N. oculata* inhibition zone, a change in the morphology of *C.*  
287 *closterium* cells in the *T. striata* inhibition zone was observed, with cells of diameter  $3.80 \pm$   
288  $0.09 \mu\text{m}$ , significantly thinner than the control culture (Mann Whitney, n=20,  $p$ -value < 0.05).  
289 No change in cell size or number of *P. purpureum* was observed when growing in Petri dishes  
290 with or without *C. closterium* as emitter (Figure 3C)

291

292

### 293 **Bacterial strains isolated from *Nannochloropsis oculata* and *Tetraselmis striata* inhibition** 294 **zones**

295

296 Six bacterial strains were identified using a Sanger approach, after isolation from the  
297 inhibition zones of *T. striata* and *N. oculata*, showing mainly small white colonies  
298 (Supplementary Table 1). In the inhibition zones of *N. oculata*, isolated bacteria were  
299 assigned to the genus *Alteromonas* sp. (sequence coverage = 100%, sequence identity =  
300 98.96%), and to the species *Alteromonas macleodii* (s.c. = 100%, s.i. = 98.02%). In the  
301 inhibition zones of *T. striata*, isolated bacteria were identified as the species *Alteromonas*  
302 *macleodii* (s.c. = 98.09 and 96.86%, s.i. = 100 and 99% respectively), as well as the genus  
303 *Lacimonas* sp (s.c. = 96.97%, s.i. = 99%). The bacterial strain *A. macleodii* isolated from the  
304 inhibition zone of the centrifuged *T. striata* biofilm supernatant was tested as an allelopathic  
305 emitter against *N. oculata* and *T. striata*, but no inhibition zone was clearly observed.

306

### 307 **The bacterial community associated with *C. closterium* biofilm**

308 Sequences analysis in metabarcoding indicated that three samples were composed of the  
309 classes: *Alphaproteobacteria*, *Bacteroidia*, and *Gammaproteobacteria*. *Alphaproteobacteria*  
310 dominated all samples with 97.3%, 87.5%, and 69.9% sequences from the one-week biofilm  
311 collected at the bottom of the tank after 14 days (March 24<sup>th</sup> 2023, referenced as 14T) and  
312 131 days of experiment (July 19<sup>th</sup> 2023, referenced as 131T), and from the three-week biofilm  
313 collected on the fabric of the roller after 131 days of experiment (July 19<sup>th</sup> 2023, referenced as  
314 131R), respectively (Fig. 4, Suppl. Table 2). *Bacteroidia* and *Gammaproteobacteria* were  
315 similarly abundant in 14T with about 1% sequences. These two classes were also similarly  
316 abundant in 131T with about 6% sequences. *Gammaproteobacteria*, however, represented  
317 more sequences than *Bacteroidia* in 131R, with 26.1% and 3.9% sequences, respectively.  
318 Among *Alphaproteobacteria*, the genus *Roseinatronobacter* dominated the three samples  
319 with 80.7%, 56.4%, and 50.9% sequences for 14T, 131R and 131T. Other genera included  
320 *Marivita*, *Oceanicaulis*, *Salinarimonas*, and a *Rhodobacteraceae* ASV, with *Marivita* and  
321 *Oceanicaulis* similarly abundant in 131R with about 10% sequences, *Rhodobacteraceae* ASV  
322 more abundant than the two genera in 14T with 13.6% sequences and *Salinarimonas* less  
323 abundant with 0.9-2.6% sequences. In *Gammaproteobacteria*, *Marinobacter* dominated all  
324 samples with 1.3%, 4.5%, and 23.7% sequences in 14T, 131T, and 131R. Less abundant  
325 genera included *Congregibacter* and *Vibrio*, as well as *Alteromonas*, which was only present  
326 in 131T. Finally, within *Bacteroidia*, *Phaeodactylibacter* was the most abundant in the  
327 samples, with 0.8%, 4.6%, and 1.7% sequences respectively in 14T, 131T and 131R. Other  
328 *Bacteroidia* included *Muricauda* and the *Schleiferiaceae* UBA7878.

329

330

### 331 **Discussion**

332 Based on inhibition tests conducted using the biofilm of *Cylindrotheca closterium* as the  
333 emitter, the growth of the two targeted microalgae strains *Nannochloropsis oculata* and  
334 *Tetraselmis striata* was suppressed and resulted in change of cell size. This finding represents  
335 evidence of growth inhibition observed among microalgae cultivated in biofilm co-cultures.  
336 Xu et al. (2019) reported previously that the diatom *C. closterium* significantly reduced the  
337 growth of the dinoflagellate *Prorocentrum donghaiense* in planktonic cocultures. They  
338 showed that extracts derived from *C. closterium* culture filtrates affected the total chlorophyll  
339 content and therefore the efficiency of photosystem II of *P. donghaiense* cells. This led to the

340 inhibition of photosynthesis and to the reduction in growth rate of this dinoflagellate species.  
341 In the present study, we observed an effect of *C. closterium* biofilm on cell size of *N. oculata*  
342 as well as of *T. striata*, where cells exhibited altered morphology (cells with deformed  
343 membranes). Other studies have also reported morphological alterations due to an allelopathic  
344 effect. For example, Pichierri et al. (2017) observed *Ostreopsis* cf. *ovata* cells with abnormal  
345 morphologies when exposed to the individual acellular filtrate from two diatoms species  
346 (*Proschkinia complanatoidea* and *Navicula* sp.), including membrane deformations and  
347 deleterious effects on the nucleus, resulting in chromatin dispersion in the cytoplasm.  
348 However, in the present study, no inhibition effect was observed from *C. closterium* the  
349 filtered biofilm supernatant at 0.2  $\mu\text{m}$ , thus without bacteria or microalgae. This suggests that  
350 compounds leading to the inhibition or death and the cell deformation of targeted algal strains  
351 were highly labile or a physical contact is required between *C. closterium* biofilm and the  
352 targets. These compounds appeared to exhibit a limited bioactive duration, likely  
353 necessitating continuous production and release during diatom cell growth or direct contact  
354 with targeted cells to optimize their efficiency. The biofilm of *C. closterium* may have been  
355 able to produce metabolites, such as observed with other microalga (Zhao et al. 2019, Long et  
356 al. 2021) capable of altering chlorophyll pigment or cytoplasmic membranes, and thereby  
357 inhibiting photosystem II, which directly impacts photosynthesis functioning. This impact on  
358 photosynthesis would lead to modifications in the cell cycle, division, and growth of the  
359 targeted microalgae, and this would explain the appearance of various morphotypes.  
360 Furthermore, we also observed in our study a significant reduction of the diameter of *C.*  
361 *closterium* when growing in the inhibition areas, which was not observed in studies focused  
362 on this diatom. Nonetheless, we could hypothesize that the production of inhibitory molecules  
363 by the *C. closterium* biofilm may represent a substantial metabolic cost, leading to a reduction  
364 in the diatom's growth (Legrand et al. 2003, Allen et al. 2016).

365 In the present study, no inhibition was observed for *Porphyridium purpureum*, a  
366 benthic microalga. The discrimination of inhibitory compounds on the target could be related  
367 to the physiology of this microalgae that possesses sulfated polysaccharide cell wall  
368 exhibiting strong antioxidant activity (Tannin-Spitz et al. 2005). This ability may protect cells  
369 against the potential damaging effects of reactive oxygen species (ROS) triggering oxidative  
370 stress under the stimulation of allelochemicals. Indeed, antialgal substances from  
371 *Cylindrotheca closterium* have been suggested to provoke oxidative stress on the  
372 dinoflagellate *Prorocentrum donghaiense* (Xu et al. 2019).

373 The bacterial strain *Alteromonas macleodii* isolated from the inhibition zone of  
374 centrifuged *Tetraselmis striata* supernatant did not show any significant antialgal activity. As  
375 *Cylindrotheca*'s biofilm and the cultures from the targeted microalgae *Tetraselmis striata*  
376 were not axenic, the isolated bacterial strains could come from either of them. In the case  
377 where *A. macleodii* came from the biofilm, it was not involved in the antialgal activity while  
378 in the case where it came from *Tetraselmis striata* culture, it was likely living in association  
379 with the algae. Like several *Gammaproteobacteria*, bacteria belonging to the genus  
380 *Alteromonas* are often found living in association with microalgae (Grossart et al. 2005, Sapp  
381 et al. 2007), such as *N. oculata* (Chernikova et al. 2020) or as competitors of *T. suecica* for  
382 nutrients (Biondi et al. 2017). The bacterial community survey of the biofilm from the tank  
383 and the roller indicated that *Alteromonas* was present in only one sample and in low sequence  
384 numbers. *Alteromonas macleodii* may form short-lived 'blooms' of active cells that are  
385 missed using traditional single-point sampling (Wietz et al. 2022). Another hypothesis could  
386 be that the isolated strain came from one of the targeted cultures instead of the *C. closterium*  
387 biofilm. The bacterial community from the one-week biofilms of the tank and the three-week  
388 biofilm of the roller fabric also contained a large majority of *Alphaproteobacteria* with the  
389 genus *Roseinatronobacter* dominating in all samples. Bacteria from the genus  
390 *Roseinatronobacter* are facultatively phototrophic purple bacteria, found in environments  
391 characterized as extreme such as alkaliphilic hypersaline lakes and are highly tolerant to large  
392 environmental gradient variations (Boldareva et al. 2007, Wilson et al. 2012, Trutschel et al.  
393 2023, Cubillos et al. 2024). Such large variations likely happen in our rotating system where  
394 bacteria are impacted in the biofilm by varying humidity conditions and salt concentrations  
395 due to evaporation. The other *Alphaproteobacteria* genera, *Marivita*, *Oceanicaulis*, and  
396 *Salinarimonas* have previously been observed associated with microalgal planktonic cultures  
397 or in algal biofilms and are believed to play a role in nutrient transformation and availability  
398 to the algae (Zhou et al. 2021, Lukwambe et al. 2023, Li et al. 2019, Cole et al. 2014, Strömpl  
399 et al. 2003). For instance, *Salinarimonas* has been shown to promote algal growth in the  
400 biofilm (Xiao et al. 2023). Within *Gammaproteobacteria*, *Marinobacter* has been identified  
401 in association with the phycosphere or the biofilm of microalgae, likely benefiting from  
402 carbon source exudates and its cells have been shown to be chemically attracted by the  
403 diatom *Thalassiosira weissflogii* (Giraldo et al. 2019, Pinto et al. 2021, Sonnenschein et al.  
404 2012). Within *Bacteroidia*, *Muricauda*, is a genus regularly found in biofilms and thought to  
405 be, as well as the genus *Marinobacter*, amongst the primary colonizers, and bacteria from this  
406 genus have been shown to play a role in cell aggregation of the microalgae *Nannochloropsis*

407 *oceanica* (Abed et al. 2019, Wang et al. 2012). *Phaeodactylibacter* bacteria are heterotrophic  
408 denitrifiers and salt tolerant, they are found in biofilms and associated with microalgae such  
409 as the diatom *Phaeodactylum tricornutum* (Chen et al. 2014, Li et al. 2021, Wang et al. 2020,  
410 Fan et al. 2023). Overall, the bacterial community associated with *C. closterium* biofilm  
411 contains genera that could play various roles such as making complex molecules available to  
412 the algae, cell aggregation or with various osmotic properties. Although the main bacterial  
413 strain isolated from the inhibition areas did not participate directly in the targeted microalgae  
414 inhibition, bacteria closely associated to *C. closterium* biofilm could have a role in the  
415 observed inhibition activity. Further analyses are needed to define the allelopathic capabilities  
416 of *C. closterium* and its microbial community in the biofilm. Additional experiments may  
417 include omics tools such as metabolomics or metatranscriptomics to identify allelochemical  
418 compounds and the metabolic pathways of the biofilm microbiota involved in algal growth  
419 inhibition. Additionally, a wider spectrum of algal targets may be tested to identify the  
420 potential allelopathic specificity of the *C. closterium* biofilm.

421

#### 422 **Funding**

423 This work was supported by the Photobiofilm Explorer project ANR-20-CE43-0008.

424

#### 425 **Competing interests**

426 The authors declare no conflict of interest.

427

#### 428 **Availability of data**

429 Partial 16S rRNA gene sequences were deposited in GenBank under the Accession number  
430 PP551695-PP551700. Raw 16S rRNA gene sequences and sample metadata are available in  
431 the SRA under BioProject ID PRJNA1098477.

432

#### 433 **Authors' contributions**

434 Conceptualization: Emilie Le Floc'h, Eric Fouilland; Methodology: Lucie Sanchez,  
435 Amandine Avouac, Emilie Le Floc'h, Christine Félix, Christophe Leboulanger, Angélique  
436 Gobet ; Formal analysis and investigation: Lucie Sanchez, Emilie Le Floc'h, Christine Félix,  
437 Angélique Gobet ; Validation: Lucie Sanchez, Emilie Le Floc'h, Christine Félix, Eric  
438 Fouilland ; Visualization : Lucie Sanchez, Emilie Le Floc'h, Angélique Gobet, Eric  
439 Fouilland ; Writing-original draft preparation: Lucie Sanchez, Eric Fouilland ; Writing-  
440 review and editing: Lucie Sanchez, Amandine Avouac, Emilie Le Floc'h, Christine Félix,

441 Christophe Leboulanger, Angélique Gobet, Eric Fouilland ; Supervision ; Emilie Le Floc'h,  
442 Christine Félix, Eric Fouilland; Funding acquisition and project administration: Eric  
443 Fouilland ; Ressources : Amandine Avouac, Emilie Le Floc'h, Christine Félix

444

#### 445 **Acknowledgments**

446 We thank the GeT-Biopuces platform, TBI (Université de Toulouse, CNRS, INRAE, INSA)  
447 and especially Lidwine Trouilh for MiSeq sequencing and Etienne Rifa for sequence  
448 processing. We also thank Eric Pruvost from LOV laboratory in Villefranche-sur-Mer,  
449 France, for providing the design of the experimental rotating system used in the present study.

450

#### 451 **References**

452

453 Abed RMM, Al Fahdi D, Muthukrishnan T (2019) Short-term succession of marine microbial  
454 fouling communities and the identification of primary and secondary colonizers.  
455 *Biofouling*, 35: 526-540.

456 Allen JL, Ten-Hage L, Leflaive J (2016) Allelopathic interactions involving benthic  
457 phototrophic microorganisms. *Env Microbiol Rep* 8: 752–762

458 Biondi N, Cheloni G, Rodolfi L, Viti C, Giovannetti L, Tredici MR (2018) *Tetraselmis*  
459 *suecica* F&M-M33 growth is influenced by its associated bacteria. *Microb Biotechnol*,  
460 11:211-223.

461 Boldareva EN, Briantseva IA, Tsapin A, Nelson K, Sorokin Dlu, Turova TP, Boïchenko VA,  
462 Stadnichuk IN, Gorlenko VM (2007) The new alkaliphilic bacteriochlorophyll a-  
463 containing bacterium *Roseinatronobacter monicus* sp. nov. from the hypersaline Soda  
464 Mono Lake (California, United States). *Mikrobiologiya*, 76: 82–92.

465 Callahan BJ, McMurdie PJ, Rosen MJ, Han AW, Johnson AJA, Holmes SP (2016). DADA2:  
466 High-resolution sample inference from Illumina amplicon data. *Nature Methods* 13:  
467 581–583.

468 Chaïb S, Pistevos JCA, Bertrand C, Bonnard (2021) Allelopathy and allelochemicals from  
469 microalgae: An innovative source for bio-herbicidal compounds and biocontrol  
470 research. *Algal Res*, 54: 102213

471 Chen Z, Lei X, Lai Q, Li Y, Zhang B, Zhang J, Zhang H, Yang L, Zheng W, Tian Y, Yu Z,  
472 Xu H, Zheng T (2014) *Phaeodactylibacter xiamenensis* gen. nov., sp. nov., a member  
473 of the family Saprospiraceae isolated from the marine alga *Phaeodactylum tricorutum*.  
474 *Int J Syst Evol Microbiol*, 64: 3496-3502.

475 Chernikova TN, Bargiela R, Toshchakov SV, Shivaraman V, Lunev EA, Yakimov MM,  
476 Thomas DN, Golyshin PN (2020) Hydrocarbon-Degrading Bacteria *Alcanivorax* and  
477 *Marinobacter* Associated With Microalgae *Pavlova lutheri* and *Nannochloropsis*  
478 *oculata*. Front Microbiol 11: 572931.

479 Cole JK, Hutchison JR, Renslow RS, Kim YM, Chrisler WB, Engelmann HE, Dohnalkova  
480 AC, Hu D, Metz TO, Fredrickson JK, Lindemann SR (2014) Phototrophic biofilm  
481 assembly in microbial-mat-derived unicyanobacterial consortia: model systems for the  
482 study of autotroph-heterotroph interactions. Front Microbiol, 5: 109.

483 Coyne KJ, Wang Y, Johnson G (2022) Algicidal Bacteria: A Review of Current Knowledge  
484 and Applications to Control Harmful Algal Blooms. Front Microbiol 13: 871177.

485 Cubillos CF, Aguilar P, Moreira D, Bertolino P, Iniesto M, Dorador C, López-García P  
486 (2024) Exploring the prokaryote-eukaryote interplay in microbial mats from an Andean  
487 athalassohaline wetland. Microbiol Spectr, 12: e0007224.

488 Edwards U, Rogall T, Blocker H, Emde M, Bottger EC (1989) Isolation and direct complete  
489 nucleotide determination of entire genes. Characterization of a gene coding for 16S  
490 ribosomal RNA. Nucl Acids Res, 17:7843–7853.

491 Flores HS, Wikfors GH, Dam HG (2012) Reactive oxygen species are linked to the toxicity  
492 of the dinoflagellate *Alexandrium* spp. to protists. Aquat Microb Ecol 66:199-209

493 Grossart H-P, Levold F, Allgaier M, Simon M, Brinkhoff T (2005) Marine diatom species  
494 harbor distinct bacterial communities. Environmental Microbiology 7: 860–873.

495 Fan G, Huang J, Jiang X, Meng W, Yang R, Guo J, Fang F, Yang J (2023) Microalgae  
496 biofilm photobioreactor and its combined process for long-term stable treatment of  
497 high-saline wastewater achieved high pollutant removal efficiency. Journal of  
498 Environmental Chemical Engineering, Volume 11: 111473.

499 Giraldo JB, Stock W, Dow L, Roef L, Willems A, Mangelinckx S, Kroth PG, Vyverman W,  
500 Michiels M (2019) Influence of the algal microbiome on biofouling during industrial  
501 cultivation of *Nannochloropsis* sp. in closed photobioreactors. Algal Research, 42:  
502 101591.

503 Guillard RRL, Ryther JH (1962) Studies of marine planktonic diatoms. I. *Cyclotella nana*  
504 Hustedt and *Detonula confervacea* Cleve. Can. J. Microbiol. 8: 229-239.

505 Guillard RRL (1975). Culture of phytoplankton for feeding marine invertebrates. In Smith  
506 WL and Chanley MH (Eds.) Culture of Marine Invertebrate Animals. Plenum Press,  
507 New York, USA, pp 26-60.

508 Gross EM (2003) Allelopathy of Aquatic Autotrophs. Crit Rev Plant Sci 22: 313-339



509 Inderjit, del Moral R (1997) Is separating resource competition from allelopathy realistic?  
510 The Botanical Review, 63: 221–230

511 Hellio C, Berge JP, Beaupoil C, Le GAL Y, Bourgougnon N (2002). Screening of Marine  
512 Algal Extracts for Anti-settlement Activities against Microalgae and Macroalgae.  
513 Biofouling, 18: 205–215.

514 Hudzicki J (2009) Kirby-Bauer Disc Diffusion Susceptibility Test Protocol. American  
515 Society for Microbiology, Washington DC: Dec 8, 2009 posting date [Online.]

516 Khairy (2010) Allelopathic effects of *Skeletonema costatum* (Bacillariophyta) exometabolites  
517 on the growth of *Nannochloropsis occulata* and *Tetraselmis chunii* (Chlorophyta). Egypt.  
518 J Exp Biol (Bot), 6: 79-85.

519 Klindworth A, Pruesse E, Schweer T, Peplies J, Quast C, Horn M, Glöckner FO (2013)  
520 Evaluation of general 16S ribosomal RNA gene PCR primers for classical and next-  
521 generation sequencing-based diversity studies. Nucleic Acids Research, 41: 1–11.

522 Leflaive J, Ten-Hage L (2007) Algal and Cyanobacterial Secondary Metabolites in  
523 Freshwaters: A Comparison of Allelopathic Compounds and Toxins. Fresh Biol 52:  
524 199-214

525 Legrand C, Rengefors K, Fistarol GO and Granéli E (2003) Allelopathy in Phytoplankton -  
526 Biochemical, Ecological and Evolutionary Aspects. Phycologia, 42: 406-419

527 Li J, Wang T, Yu S, Bai J, Qin S (2019) Community characteristics and ecological roles of  
528 bacterial biofilms associated with various algal settlements on coastal reefs. J Environ  
529 Manage, 250: 109459.

530 Li Y, Wu Y, Wang S, Jia L (2021) Effect of organic loading on phosphorus forms  
531 transformation and microbial community in continuous-flow A2/O process. Water Sci  
532 Technol, 83: 2640-2651.

533 Long M, Peltekis A, González-Fernández C, Hégaret H, Bailleul B (2021) Allelochemicals of  
534 *Alexandrium minutum*: Kinetics of membrane disruption and photosynthesis inhibition  
535 in a co-occurring diatom. Harmful Algae, 103:101997.

536 Lukwambe B, Nicholous R, Zheng Z (2024) The functional diversity of microbial  
537 communities in the multi-compartment biofilters of shrimp mariculture effluents using  
538 16S rRNA metabarcoding. Aquacult Int, 32: 1081–1099.

539 Morales M, Bonnefond H, Bernard O (2020) Rotating algal biofilm versus planktonic  
540 cultivation: LCA perspective. J Cleaner Prod 254: 120547

541 Parks DH, Chuvochina M, Rinke C, Mussig AJ, Chaumeil P-A, Hugenholtz P (2022) GTDB:  
542 An ongoing census of bacterial and archaeal diversity through a phylogenetically

543 consistent, rank normalized and complete genome-based taxonomy. *Nucleic Acids*  
544 *Research* 50: D785–D794.

545 Pascon G, Messina M, Petit L, Pinheiro Valente LM, Oliveira B, Przybyla C, Dutto G and  
546 Tulli F (2021) Potential application and beneficial effects of a marine microalgal  
547 biomass produced in a high-rate algal pond (HRAP) in diets of European sea bass,  
548 *Dicentrarchus labrax*. *Env Sci Pollut Res* 28: 62185–62199

549 Penaranda D, Bonnefond H, Guihéneuf F, Morales M, Bernard O (2023) Life cycle  
550 assessment of an innovative rotating biofilm technology for microalgae production: An  
551 eco-design approach. *J Cleaner Prod* 384: 135600

552 Pichierri S, Accoroni S, Pezzolesi L, Guerrini F, Romagnoli T, Pistocchi R, Totti C (2017)  
553 Allelopathic effects of diatom filtrates on the toxic benthic dinoflagellate *Ostreopsis* cf.  
554 *ovata*. *Mar Environ Res*, 131:116-122.

555 Pinto J, Lami R, Krasovec M, Grimaud R, Urios L, Lupette J, Escande ML, Sanchez F,  
556 Intertaglia L, Grimsley N, Piganeau G, Sanchez-Brosseau S (2021) Features of the  
557 Opportunistic Behaviour of the Marine Bacterium *Marinobacter algicola* in the  
558 Microalga *Ostreococcus tauri* Phycosphere. *Microorganisms* 9: 1777.

559 Quast C, Pruesse E, Yilmaz P, Gerken J, Schweer T, Yarza P, Peplies J, Glöckner FO (2013).  
560 The SILVA ribosomal RNA gene database project: Improved data processing and web-  
561 based tools. *Nucleic Acids Research* 41: 590–596.

562 R Core Team (2021) R: A Language and Environment for Statistical Computing.  
563 <http://www.r-project.org/>

564 Sapp M, Schwaderer AS, Wiltshire KH, Hoppe H-G, Gerdts G, Wichels A (2007) Species-  
565 specific bacterial communities in the phycosphere of microalgae. *Microbial Ecology* 53:  
566 683–699.

567 Sonnenschein EC, Syit DA, Grossart HP, Ullrich MS (2012) Chemotaxis of *Marinobacter*  
568 *adhaerens* and its impact on attachment to the diatom *Thalassiosira weissflogii*. *Appl*  
569 *Environ Microbiol*, 78: 6900-7.

570 Stackebrandt E, Liesack W (1993) Nucleic acids and classification. In: Handbook of new  
571 bacterial systematics, pp. 151- 194. Academic Press Ltd., London.

572 Strömpl C, Hold GL, Lünsdorf H, Graham J, Gallacher S, Abraham WR, Moore ER, Timmis  
573 KN (2003) *Oceanicaulis alexandrii* gen. nov., sp. nov., a novel stalked bacterium  
574 isolated from a culture of the dinoflagellate *Alexandrium tamarense* (Lebour) Balech.  
575 *Int J Syst Evol Microbiol*, 53:1901-6.

576 Tannin-Spitz T, Bergman M, van Moppes D, Grossman S, Arad SM (2005) Antioxidant  
577 activity of the polysaccharide of the red microalga *Porphyridium* sp. J Appl Phycol,  
578 17:215–222.

579 Thomas F, Dittami SM, Brunet M, Le Duff N, Tanguy G, Leblanc C Gobet A (2020).  
580 Evaluation of a new primer combination to minimize plastid contamination in 16S  
581 rDNA metabarcoding analyses of alga-associated bacterial communities.  
582 Environmental Microbiology Reports, 12: 30–37.

583 Trefault N, De La Iglesia R. Moreno-Pino M, Lopes Dos Santos A, Gérikas Ribeiro C,  
584 Parada-Pozo G, Cristi A, Marie D, Vaultot D (2021) Annual phytoplankton dynamics in  
585 coastal waters from Fildes Bay, Western Antarctic Peninsula. Scientific Reports, 11:  
586 1368.

587 Trutschel LR, Rowe AR, Sackett JD (2023) Complete genome sequence of  
588 *Roseinatronobacter* sp. strain S2, a chemolithoheterotroph isolated from a pH 12  
589 serpentinizing system. Microbiol Resour Announc, 12: e0028823.

590 Uchida T (2001) The role of cell contact in the life cycle of some dinoflagellate species. J  
591 Plankton Res 23: 889–891

592 Vallina SM, Follows MJ, Dutkiewicz S, Montoya JM, Cermeno P, Loreau M (2014) Global  
593 relationship between phytoplankton diversity and productivity in the ocean. Nature  
594 Communications 5: 4299

595 Wang H, Laughinghouse HD 4th, Anderson MA, Chen F, Williams E, Place AR, Zmora O,  
596 Zohar Y, Zheng T, Hill RT (2012) Novel bacterial isolate from Permian groundwater,  
597 capable of aggregating potential biofuel-producing microalga *Nannochloropsis*  
598 *oceanica* IMET1. Appl Environ Microbiol, 78:1445-53.

599 Wang J, Zhou J, Wang Y, Wen Y, He L, He Q (2020) Efficient nitrogen removal in a  
600 modified sequencing batch biofilm reactor treating hypersaline mustard tuber  
601 wastewater: The potential multiple pathways and key microorganisms. Water Res, 177:  
602 115734.

603 Wietz M, López-Pérez M, Sher D, Biller SJ, Rodriguez-Valera F (2022) Microbe Profile:  
604 *Alteromonas macleodii* - a widespread, fast-responding, 'interactive' marine bacterium.  
605 Microbiology (Reading), 168: 001236.

606 Wenjing X, Wang J, Tan L, Guo X, Xue Q (2019) Variation in Allelopathy of Extracellular  
607 Compounds Produced by *Cylindrotheca Closterium* against the Harmful-Algal-Bloom  
608 Dinoflagellate *Prorocentrum Donghaiense*. Mar Env Res 148: 19-25

609 Wilson SL, Frazer C, Cumming BF, Nuin PA, Walker VK (2012) Cross-tolerance between  
610 osmotic and freeze-thaw stress in microbial assemblages from temperate lakes. *FEMS*  
611 *Microbiol Ecol* 82: 405-15.

612 Xiao C, Yuan J, Li L, Zhong N, Zhong D, Xie Q, Chang H, Xu Y, He X, Li M (2022)  
613 Photocatalytic synergistic biofilms enhance tetracycline degradation and conversion.  
614 *Environ Sci Ecotechnol*, 4: 100234.

615 Xu W, Tan L, Guo X, Wang J (2019) Isolation of anti-algal substances from *Cylindrotheca*  
616 *closterium* and their inhibition activity on bloom-forming *Prorocentrum donghaiense*.  
617 *Ecotox Environ Safety* 190: 110180

618 Zhao JX, Yang L, Zhou Lv, Bai Y, Wang B, Hou P, Xu Q, Yang W, Zuo Z (2019) Inhibitory  
619 effects of eucalyptol and limonene on the photosynthetic abilities in *Chlorella vulgaris*  
620 (Chlorophyceae). *Phycologia* 55: 696-702

621 Zhou X, Zhang XA, Jiang ZW, Yang X, Zhang XL, Yang Q (2021) Combined  
622 characterization of a new member of *Marivita cryptomonadis* strain LZ-15-2 isolated  
623 from cultivable phycosphere microbiota of highly toxic HAB dinoflagellate  
624 *Alexandrium catenella* LZT09. *Braz J Microbiol*, 52: 739–748.

625

626 **Tables**

627

628 **Table 1:** Results obtained of the inhibition test conducted after 15 days of incubation under  
 629 continuous light with *Nannochloropsis oculata*, *Tetraselmis striata* and *Porphyridium*  
 630 *purpureum* as the targeted microalgae strain and *Cyclindrotheca closterium* in biofilm  
 631 (harvested from the bottom of the tank or from the fabric of the roller) acting as the emitter  
 632 when (i) the whole biofilm, (ii) the centrifuged biofilm pellet, and (iii) the centrifuged biofilm  
 633 supernatant filtered or not, incubated after 14 and 131 days of experiment using the rotating  
 634 system. Results are expressed as the percentage (%) of the inhibition zone measured around  
 635 the diffusion discs with the emitter relative to the inhibition zone measured with hydrogen  
 636 peroxide as the positive control. Mean and range from replicates (n=2) are reported.

Days of Experiment	Target species	One-week old biofilm from the bottom of the tank			Three-week old biofilm from the roller fabric			
		Whole biofilm	centrifuged biofilm pellet	centrifuged biofilm supernatant	Whole biofilm	centrifuged biofilm pellet	centrifuged biofilm supernatant	filtered centrifuged biofilm supernatant
14 days (March 24th 2023)	<i>N. oculata</i>	150 (±16)	91 (±60)	158 (±43)	not tested	not tested	not tested	not tested
	<i>T. striata</i>	33 (±5)	24 (±10)	33 (±2)	not tested	not tested	not tested	not tested
	<i>P. purpureum</i>	0	0	0	not tested	not tested	not tested	not tested
131 days (July 19th 2023)	<i>N. oculata</i>	65 (±21)	not tested	not tested	39 (±10)	16 (±4)	26 (±26)	0
	<i>T. striata</i>	92 (±19)	not tested	not tested	12 (±6)	18 (±18)	38 (±14)	0
	<i>P. purpureum</i>	0	not tested	not tested	0	0	0	0

637

638

639

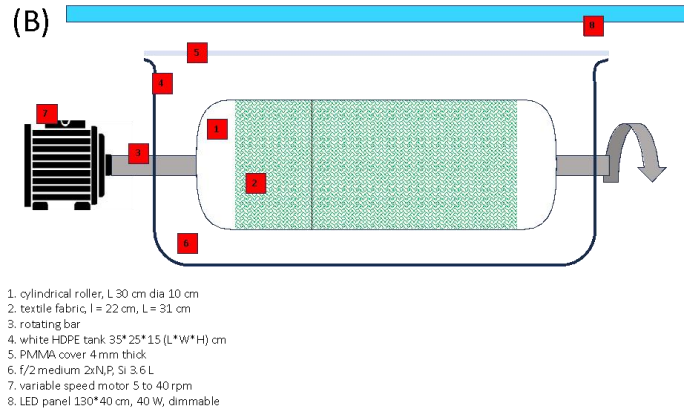
640 **Table 2.** Identification of bacterial colonies isolated from inhibition zones of the targeted  
 641 microalgae around the biofilm type, from the one-week biofilm growing at bottom of the tank  
 642 collected on March 19<sup>th</sup> 2023. Details on sequence taxonomic identification are available in  
 643 Supplementary Table 2.

644

Inhibition zone from the targeted microalga	Putative bacterial species	16S rDNA sequence length (bp)	Sequence coverage (%)	Sequence identity (%)	Accession number of the best hit	
<i>N. oculata</i>	centrifuged biofilm supernant	<i>Alteromonas macleodii</i>	858	100%	98.02%	MT325885.1
	whole biofilm	<i>Alteromonas</i> sp.	1094	100%	98.17%	MT210817.1
	whole biofilm	<i>Alteromonas</i> sp.	772	100%	98.96%	MF599947.1
<i>T. striata</i>	centrifuged biofilm supernant	<i>Alteromonas macleodii</i>	941	100%	98.09%	MT325885.1
	whole biofilm	<i>Alteromonas macleodii</i>	834	99%	96.86%	HM584088.1
	whole biofilm	<i>Lacimonas</i> sp.	860	99%	96.97%	MK493541.1

645

646

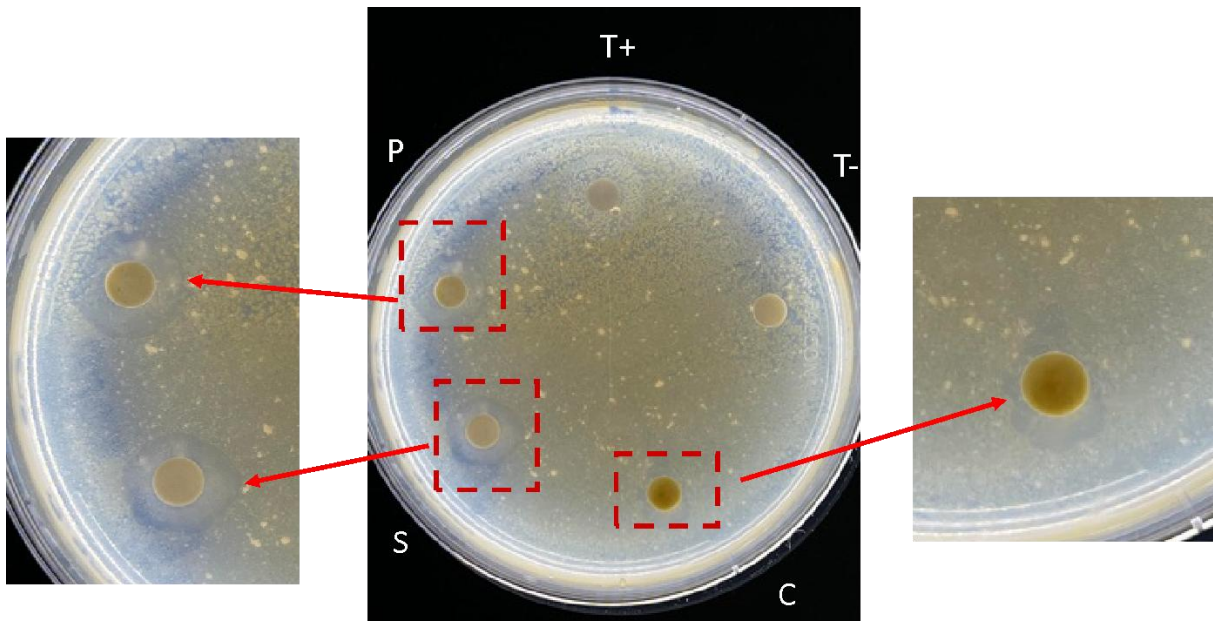


647

648 Figure 1: *Cylindrotheca closterium* growing as biofilm (A) using an experimental rotating  
 649 culture system described in (B)

650

651

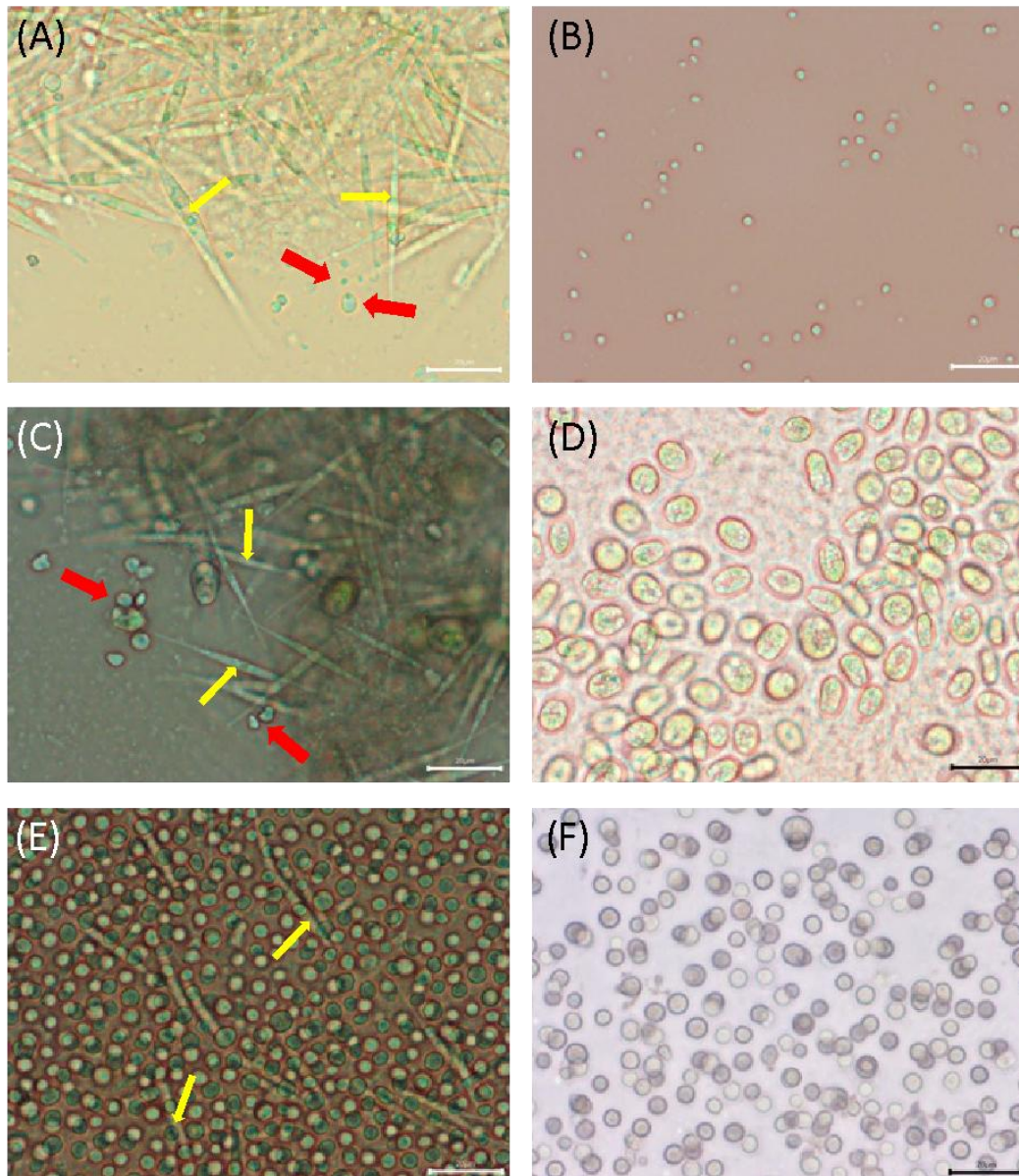


652

653 Figure 2: Result of one inhibition test using *Cylindrotheca closterium* one-week biofilm from  
 654 the bottom of the tank (March 19<sup>th</sup> 2023) against the target *Nannochloropsis oculata*. T+:  
 655 hydrogen peroxide, T-: sterile modified f/2 medium, P: paste from the one-week biofilm at  
 656 the bottom of the tank, C: pellet obtained from centrifugation of the biofilm, and S:  
 657 supernatant obtained from the centrifugation of the biofilm. Inhibition zones were observed  
 658 after 15 days of incubation at 20 °C under continuous neutral light at an intensity of 80-90  
 659  $\mu\text{mol photons.m}^{-2}.\text{s}^{-1}$ .

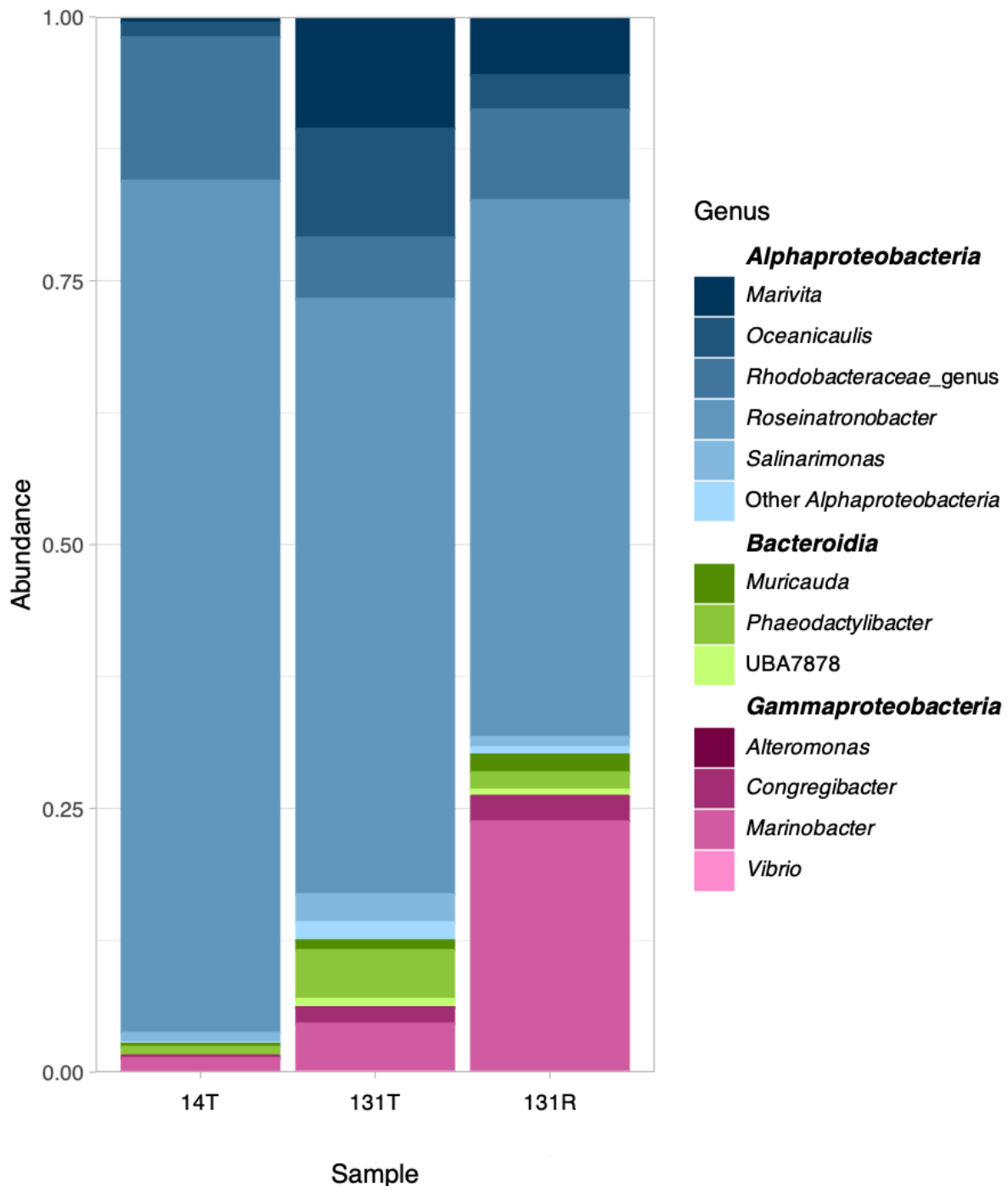
660

661



662

663 Figure 3: Observation under an inverted microscope of (A) *N. oculata* sampled from the  
 664 inhibition zone with the one-week centrifuged *C. closterium* biofilm supernatant collected  
 665 from the bottom of the tank (March 24<sup>th</sup> 2023) as the emitter, (B) *N. oculata* sampled from  
 666 control cultures in Petri dish with no emitters, (C) *T. striata* sampled from the inhibition zone  
 667 with the one-week centrifuged *C. closterium* biofilm supernatant collected from the bottom of  
 668 the tank (March 24<sup>th</sup> 2023) as the emitter, (D) *T. striata* sampled from control cultures in Petri  
 669 dish with no emitters, (E) *P. purpureum* sampled from the inhibition zone with the one-week  
 670 centrifuged *C. closterium* biofilm supernatant collected from the bottom of the tank (March  
 671 24<sup>th</sup> 2023) as the emitter, (F) *P. purpureum* sampled from control culture in Petri dish with no  
 672 emitters. Deformed cells are indicated by red arrows. *C. closterium* cells are indicated by  
 673 yellow arrows.



674

675 Figure 4 : Taxonomic composition of the bacterial community at the genus level, classified at  
 676 the class level, in the 3 samples. Other *Alphaproteobacteria*, *Alphaproteobacteria* genera with  
 677 less sequences than the five most abundant genera in the dataset. (14T: One-week biofilm  
 678 collected from the bottom of the tank after 14 days of experiment (March 24<sup>th</sup> 2023), 131T:  
 679 One-week biofilm collected from the bottom of the tank after 131 days of experiment (July  
 680 19<sup>th</sup> 2023), 131R: One-week biofilm collected from the fabric of the roller after 131 days of  
 681 experiment (July 24<sup>th</sup> 2023). Details on sequence taxonomic identification are available in  
 682 Supplementary Table 3.